BLOS1, a putative BLOC-1 subunit, interacts with SNX1 and modulates root growth in *Arabidopsis*

Yanyan Cui[1,2], Xugang Li[3], Qingguo Chen[1,2], Xin He[1], Qing Yang[1,2], Aili Zhang[1,2], Xin Yu[3], Hao Chen[1,2], Naiyou Liu[1], Qi Xie[1], Weicai Yang[1], Jianru Zuo[1], Klaus Palme[3,*] and Wei Li[1,*]

[1]Key Laboratory of Molecular Developmental Biology, Institute of Genetics and Developmental Biology, Chinese Academy of Sciences, Beijing 100101, China
[2]Graduate School of Chinese Academy of Sciences, Beijing 100039, China
[3]Institut für Biologie II, Universität Freiburg, 79104 Freiburg, Germany
*Authors for correspondence (wli@genetics.ac.cn; klaus.palme@biologie.uni-freiburg.de)

Summary

Internalization and sorting of macromolecules are inherent properties of all eukaryotic cells that are achieved by vesicle trafficking. However, this process is relatively less understood in plants. An eight-subunit protein complex, BLOC-1, which is involved in endosomal transport from the endosomes to the lysosomes, has been identified in both human and mice. In this study, two homologous subunits of this complex, BLOS1 (or AtGCN5L1) and BLOS2, have been characterized in *Arabidopsis*. Both BLOS1 and BLOS2 interacted with SNX1 on the sorting endosomes. Inducible RNAi lines with reduced levels of BLOS1 had longer primary roots and more lateral roots. Consistently, PIN1 and PIN2 were increased in *BLOS1* RNAi lines, implicating an impaired transport from the endosomes to the vacuoles. These results suggest that a putative BLOC-1 complex in *Arabidopsis* might mediate the vacuolar degradative transport through direct interaction with SNX1 to regulate the homeostasis of PIN1 and PIN2, which is important for plant growth and development.

Key words: Biogenesis of lysosome-related organelles complex 1 (BLOC-1), Sorting nexin 1 (SNX1), Auxin efflux transporter, Root growth, Endosomal transport, Vacuole

Introduction

Vesicle trafficking performs conserved functions in eukaryotes. It is involved in communication among different cell compartments and the exchange of information between cells and their environment. Endosomal transport plays a central role in vesicle trafficking as it connects anterograde transport from the Golgi apparatus to the endosomes and the lysosomes, endocytic transport from the plasma membrane to the endosomes and retrograde transport from the endosomes to the Golgi (Bonifacino and Rojas, 2006; Li et al., 2007). Cargo is sorted from the early endosomes to the cell surface, recycling endosomes or late endosomes and lysosomes (Gruenberg, 2001; Bonifacino and Glick, 2004). Components destined for the lysosomes are sorted to the late endosomes, or multivesicular bodies, which contain whorls of membranes and vesicles. The late endosomes morph into the lysosomes with a highly regulated fusion machinery (Raposo et al., 2007). The lysosomes serve as the major degradative compartments in eukaryotic cells (Kornfeld and Mellman, 1989). In addition, the secretory lysosomes or some specialized lysosome-related organelles play important functions in secretion via exocytosis (Raposo et al., 2007).

In contrast to mammalian cells, plant vesicle trafficking is less well understood. The identification of genes encoding components of vesicle trafficking in plant genomes suggests the conserved role of vesicle trafficking in plants. Endosomal transport plays a key role in many processes in plants including embryo differentiation (Goh et al., 2007; Silady et al., 2008), cell fate specification (Shen et al., 2003; Tian et al., 2007), cell wall remodeling (Baluska et al., 2002), gravitropism (Silady et al., 2004; Abas et al., 2006) and polar auxin transport (Gälweiler et al., 1998; Steinmann et al.,

1999; Geldner et al., 2001; Jallais et al., 2006; Jallais et al., 2007; Jallais et al., 2008; Dhonukshe et al., 2008). Endosomal trafficking is essential for polar transport of the phytohormone auxin and its influx (AUX) and efflux (PIN) carriers (Paciorek et al., 2005; Müller et al., 2007). Targeting of PIN1 protein to the basal plasma membrane requires PIN1 recycling from the plasma membrane to the endosomes mediated by GNOM, an endosomal GDP and GTP exchange factor for ARF GTPases (Geldner et al., 2003). By contrast, PIN2 transport requires the SNX1-positive endosomes. SNX1 is a newly described plant-sorting nexin that is localized to the prevacuolar compartment (PVC) in plants (Jaillais et al., 2006). Besides SNX1, another component of retromer, VPS29, is proposed to function in endosomal recycling of PINs. In the *vps29* mutant, intracellular accumulation of PIN1 and, to a lesser degree, of PIN2 and other membrane proteins was observed. VPS29 colocalizes with SNX1 and is required for maintaining the SNX1 endosomal morphology but not the GNOM endosomes. A current model is that PINs are internalized first through the GNOM endosomes and then routed to the SNX1 endosomes for recycling (Jaillais et al., 2007). Nevertheless, the destination of the endocytosed PIN1 and PIN2 remains to be clarified.

It has been demonstrated that plants have evolved different vacuoles to adapt their metabolism. Vacuoles, including the protein storage vacuole (PSV) and the lytic vacuole (LV), are important structures in vesicle trafficking. The lytic vacuoles share lysosome-like properties but also function as the protein storage vacuoles for protein accumulation (Frigerio et al., 2008). LVs and PSVs have different pH in their lumen, as highlighted by staining with pH- or acidic protease-sensitive dyes. The general consensus stemming from extensive tonoplast intrinsic protein (TIP) isoform analysis is

that α-TIP is enriched in PSVs, γ-TIP in LVs and δ-TIP in storage vacuoles (Jauh et al., 1998; Jauh et al., 1999). However, the transport machinery of cargoes from the endosomes to LVs or PSVs is lacking. Meanwhile, the physiological role of LVs in the maintenance of the steady-state levels of the endocytosed proteins remains to be elucidated.

The BLOC-1 complex consists of at least eight subunits in both human and mice, including dysbindin, snapin, muted, pallidin, cappuccino, BLOS1, BLOS2 and BLOS3. It is involved in vesicle trafficking from the endosomes to the lysosomes in higher eukaryotes (Li et al., 2007; Raposo et al., 2007; Truschel et al., 2009). Human Hermansky-Pudlak syndrome (HPS) is caused by the mutations of genes encoding dysbindin or BLOS3 (Li et al., 2003; Morgan et al., 2006). HPS is characterized by the defects in the biogenesis of lysosome-related organelles due to impaired cargo transport from the endosomes to the lysosomes (Li et al., 2007; Raposo et al., 2007). Whether there exists a homologous BLOC-1 complex in plants is unknown. Sequence comparisons reveal putative homologs of BLOS1 (also known as AtGCN5L1) and BLOS2 in *Arabidopsis*. Whether these homologs play similar roles in endosomal transport in *Arabidopsis* requires investigation. We here report the first evidence of a putative BLOC-1 in *Arabidopsis* and its possible involvement in the transport of PIN1 and PIN2, mediated by SNX1, to control root development.

Results

BLOS1 and BLOS2 are putative homologs of mammalian BLOC-1 subunits

Multiple protein sequences from different species were aligned using the ClustalW2 program (http://www.ebi.ac.uk/Tools/clustalw2/) and GeneDoc (http://www.nrbsc.org/downloads/) (supplementary material Fig. S1). The percentage of identity between the *Arabidopsis* and human proteins was calculated using the BLASTP algorithm (http://blast.ncbi.nlm.nih.gov/). The calculated sequence identities to human homologs for *BLOS1* (At2g30330) and *BLOS2* (At5g49550) were 36% and 29%, respectively. Interaction between BLOS2 and BLOS1 was revealed by yeast two-hybrid assays (Fig. 1A) and split-YFP assays (Fig. 1B). Next, our work is mainly focused on the functional studies of BLOS1.

BLOS1 is expressed in multiple tissues

Tissue-specific expression of *BLOS1* was tested by real-time PCR with RNA extracted from adult plants. *BLOS1* expression was found in all major tested organs including the root, stem, leaf, flower and silique, with highest expression in the leaf (Fig. 1C). Western blotting by a polyclonal anti-BLOS1 antibody was consistent with these findings (Fig. 1D).

Tissue-specific expression of *BLOS1* promoter activity was further analyzed by histochemical localization of GUS activity. In 5-day-old germinating seedlings, *GUS* expression was detected in the vascular tissues (Fig. 2A), shoot apical meristem (Fig. 2B) and primary root (Fig. 2C). At 9 days, *GUS* expression was clearly detectable in the adventitious root (Fig. 2D) and the lateral root primordia (Fig. 2E). GUS activity in up to 4-week-old transgenic *BLOS1* pro::GUS seedlings showed expression in the flowers, anthers and silique (Fig. 2F–H).

BLOS1 is partially localized to the endosomal compartments

To study the subcellular localization of BLOS1, a protoplast system was adopted. Sixteen hours after cotransformation with different
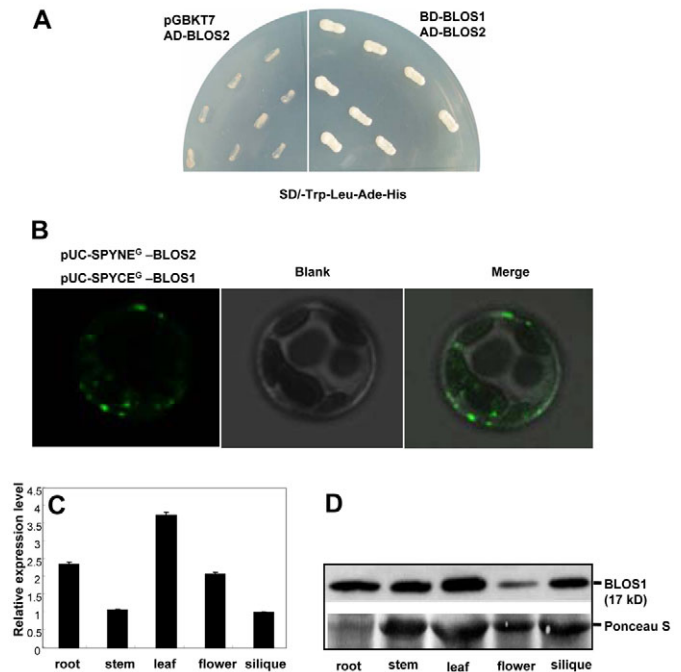

Fig. 1. BLOS1 interacts with BLOS2 and is expressed in multiple tissues. (**A**) Interaction between BLOS1 and BLOS2 in yeast two-hybrid assays. BLOS2 exhibits directional interactions with BLOS1. No interaction is detected between BLOS2 and the empty pGBKT7 vector. (**B**) BLOS1 and BLOS2 interaction in a split-YFP system. Subcloning of BLOS1 and BLOS2 into split-YFP gateway vectors pUC-SPYCE[G]–BLOS1 and pUC-SPYNE[G]–BLOS2 forms YFP C-terminal and N-terminal fusion proteins, respectively. (**C**) Tissue expression of BLOS1 in adult plants by real-time PCR. *BLOS1* mRNA levels in wild-type plants were determined by real-time PCR using gene-specific primers and total RNA from the root, stem, leaf, flower and silique. Actin is used as an internal control. BLOS1 is expressed in all these tissues with different levels. Experiments were repeated three times independently. (**D**) Western blotting assay of BLOS1 in different tissues. Protein extract from the root, stem, leaf, flower and silique were loaded to 12% SDS-PAGE for separation and probed by purified BLOS1 antibody. Ponceau S staining was used as loading control.

organellar markers, confocal images showed that BLOS1 partially colocalized with endosome markers ARA7 (Fig. 3A) and VAMP727 (Fig. 3B), PVC and vacuole markers PEP72 (Fig. 3C) and VAM3 (Fig. 3D). These data indicate that BLOS1 is probably localized at the endosomal compartments.

Altered root phenotypes in *BLOS1* RNAi knockdown lines

Histochemical GUS staining suggested that BLOS1 might play a role in root development. As there is no T-DNA exonal insertion line available, an XVE-inducible RNAi construct was made to specifically knockdown *BLOS1*. *BLOS1* full-length cDNA was subcloned into an XVE vector to produce sense and antisense strands. Western blotting showed that the protein level of BLOS1 in RNAi line L4 was apparently lower than that in the wild type after estradiol inducement (Fig. 4A), which is consistent with the lower level of *BLOS1* transcripts by northern blotting after estradiol inducement (data not shown). Our work focused on root phenotype analysis in transgenic line L4, although phenotypes in other tissues might exist. The knockdown line L4 had longer primary roots and more lateral roots (Fig. 4B,C).
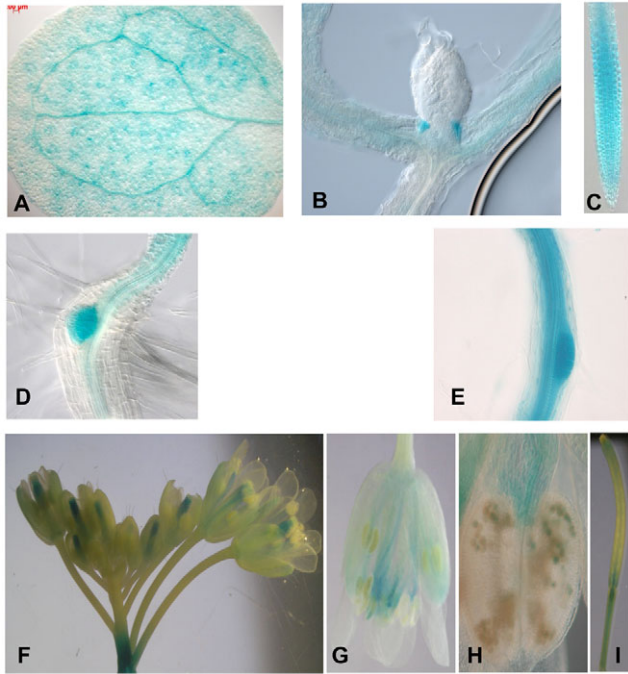
Fig. 2. Temporal and spatial expression patterns of BLOS1. GUS staining of BLOS1 is detected in the leaf vein, shoot apex and primary root in 5-day-old seedlings (**A–C**), the adventitious root and lateral root primordial in 9-day-old seedlings (**D**,**E**) and the pistil, stamen, anther and silique of 4-week-old seedlings (**F–I**).

Fig. 3. Subcellular distribution of BLOS1 in protoplasts. Pictures show the images of cotransformation of *BLOS1* with endosome markers ARA7 (**A**) and VAMP727 (**B**), and PVC to vacuole markers PEP72 (**C**) and VAM3 (**D**). Red, *BLOS1*-DsRed; green, organelle markers.

BLOS1 interacted with SNX1

To explore the function of BLOS1, full-length *BLOS1* cDNA was used as a bait to screen an *Arabidopsis* cDNA library. SNX1 (At5g06140) was identified as a novel interactor (Fig. 5A) via the GCN5L domain of BLOS1 (Fig. 5B). Likewise, BLOS2 interacted with SNX1 in the yeast two-hybrid assay (Fig. 5C), further supporting that BLOS1 and BLOS2 might function in the same complex. In addition, BLOS1 and SNX1 colocalized in protoplast (Fig. 5D). To further confirm this interaction, we found that BLOS1 interacted with SNX1 in onion and protoplast by split-YFP assays (Fig. 5E,F).

Increase of PIN1 and PIN2 in *BLOS1* RNAi lines

Considering a possible role for BLOS1 in endosomal trafficking, we hypothesized that BLOS1 recruits PINs sorted by SNX1 and transports a portion of PINs to the vacuoles for degradation. Immunocytochemical analysis of PIN1 and PIN2 in *BLOS1* RNAi knockdown lines showed that the protein levels of PIN1 and PIN2 on the plasma membrane increased after inducement (Fig. 6C,D) compared with wild type (Col-0) after inducement (Fig. 6A,B). However, the polar distributions of both PIN1 and PIN2 were not apparently altered. To rule out the possibility of transcriptional upregulation of PIN1 and PIN2 by BLOS1, we performed real-time PCR and the results showed no significant increase of *PIN1* or *PIN2* transcripts in the *BLOS1* RNAi-L4 after inducement by estradiol (Fig. 6E).

To further study whether the accumulation of PIN1 and PIN2 on the plasma membrane is due to a defect in the endocytosis of these PINs, the recruitment to the endosomes after tracing for 15 minutes in L4 was examined. Recruitment was not apparently impaired as
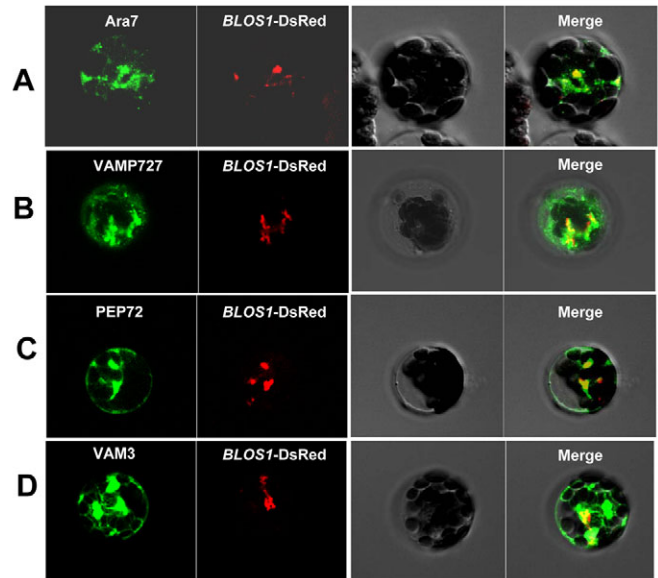
controlled by the effects of brefeldin A (BFA) treatment in FM4-64 endocytic assays (Fig. 7), suggesting that the endocytosis of PIN proteins from the plasma membrane to the endosomes might not be affected in these lines.

Discussion

Although the cellular function of the endosomal transport complex BLOC-1 in mammals requires further definition (Li et al., 2007), we here provide the first report of its possible involvement in endosomal trafficking in plants. BLOS1 and BLOS2 in *Arabidopsis* are probably two homologous subunits of BLOC-1, as revealed by sequence comparison, biochemical features and cellular function in endosomal transport. Downregulation of BLOS1 causes longer primary and lateral roots, suggesting that the homologous BLOC-1 complex might be involved in root development by negatively regulating the stability of PIN1 and PIN2 through the interaction with SNX1.

Thus far, at least eight subunits have been identified in the mammalian BLOC-1 complex, which is involved in cargo-specific sorting from the endosomes to the lysosomes (Li et al., 2007; Setty et al., 2007; Truschel et al., 2009). Sequence comparison reveals only two putative homologs (BLOS1 and BLOS2) of BLOC-1 subunits in *Arabidopsis*. Whether the composition of BLOC-1 is the same as its mammalian counterpart remains to be characterized biochemically. As shown in this study, BLOS1 and BLOS2 interact directly, suggesting a conservative role of BLOC-1 in protein trafficking from the endosome to the vacuole in plants.

Cargo sorting from the trans-Golgi network (TGN) or from the plasma membrane (PM) to the lysosomes might share similar machinery. It is evident that BLOC-1 directs cargoes from the TGN or from the PM to the lysosome-related organelles or to the lysosomes for degradation (Setty et al., 2007; Iizuka et al., 2007; Truschel et al., 2009). In *Arabidopsis*, it is known that PIN proteins rapidly and constitutively cycle between the PM and the endosomes
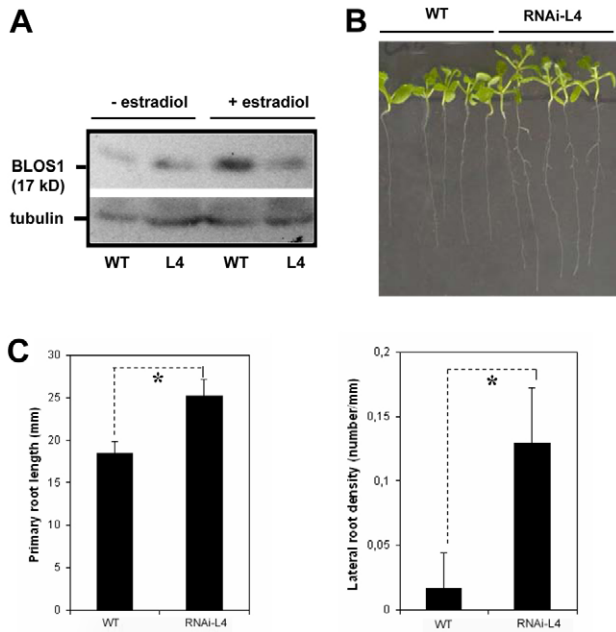
Fig. 4. Altered root phenotypes in *BLOS1* RNAi knockdown lines.
(**A**) Western blot analysis of RNAi line L4 probed with anti-BLOS1 antibody. Experiments are carried out by using both wild-type (WT, Col-0) and transgenic plants treated with estradiol or DMSO. Note that the quantity of BLOS1 decreased after inducement with estradiol in the L4 line. (**B**,**C**) Root phenotypes of the *BLOS1* transgenic line 4. Phenotype comparisons are shown between wild-type *Arabidopsis* and RNAi line L4. Primary root length and lateral root density of 8-day-old seedlings from the wild-type and transgenic lines are counted. All plants grow vertically with $10\,\mu M$ beta-estradiol in vitro. Data shown are the averages + s.d. of 20 seedlings. *$P<0.05$.

Fig. 5. Interactions between BLOS1 and SNX1. (**A**) BLOS1 interacts with SNX1 in yeast cells. Transformants containing pGBKT7-BLOS1 and pGADT7-SNX1 grow in high-stringency medium. (**B**) Interaction between the GCN5L domain of BLOS1 and SNX1. Transformants of pGBKT7-BLOS1-GCN5L and pGADT7-SNX1 grow on a SD/-Trp-Leu-Ade-His plate, whereas the remaining part of BLOS1 (NT) does not grow in this high-stringency medium. (**C**) Interaction between BLOS2 and SNX1 in yeast two-hybrid assays. BLOS2 exhibits direction interactions with SNX1. No interaction is detected between BLOS2 and the empty pGBKT7 vector. (**D**) BLOS1-DsRed and SNX1-GFP are partially colocalized in transiently transformed protoplast. Green, SNX1-GFP; red, BLOS1-DsRed. (**E**) BLOS1 interacts with SNX1 in onion. pUC-SPYCE-BLOS1 and pUC-SPYNE-SNX1 are coated with gold particles. The onion (*Allium cepa*) epidermis is peeled and bombarded using a gene gun. The bombarded samples are incubated on MS plates at 28°C for 24 hours before confocal observation. (**F**) BLOS1 interacts with SNX1 in protoplast. pUC-SPYCE^{G}-BLOS1 and pUC-SPYNE^{G}-SNX1 are cotransformed to protoplast as described previously. After incubation in 23°C for 16 hours, YFP fluorescent signal was imaged by laser-scanning confocal microscopy.

(Geldner et al., 2001). Internalization of PIN2 is clathrin-mediated (Dhonukshe et al., 2007) and it is then transferred to the sorting endosomes via SNX1 (Jaillais et al., 2006). However, the destination of the internalized PIN proteins remains uncertain. One possibility is the temporary storage in specific vesicles for fast recycling to the PM. Another possible fate is the proteasomal degradation of ubiquitinated PINs (Abas et al., 2006). Third, there is evidence that PINs could be targeted for vacuolar degradation in the absence of light (Laxmi et al., 2008), which might be mediated by the ESCRT complex (Spitzer et al., 2009). Nevertheless, the molecular aspects of this route are primitive. Currently, there are no direct interactions reported among the PINs, SNX1 and ESCRT. Here, we show for the first time physical interactions between SNX1 and BLOS1/2, which might provide insights into the complexity of PIN protein homeostasis.

It is probable that a portion of PIN proteins could be targeted for vacuolar degradation mediated by SNX1 and BLOS1/2, suggesting a conservative role of BLOC-1 in mammals and plants for vacuolar targeting. First, both BLOS1 and BLOS2 interact with SNX1, which probably occurs within the endosomal compartments. Second, SNX1 is reported to mediate PIN2 transport (Jaillais et al., 2006). Third, knockdown of *BLOS1* leads to an increase of PIN1 and PIN2, which is probably caused by impaired vacuolar degradation as discussed below.

The augmentation of PIN1 and PIN2 could be a result of: (1) transcriptional upregulation of PIN1 and PIN2 by BLOS1; (2) impaired endocytosis of PIN1 and PIN2; and (3) delayed
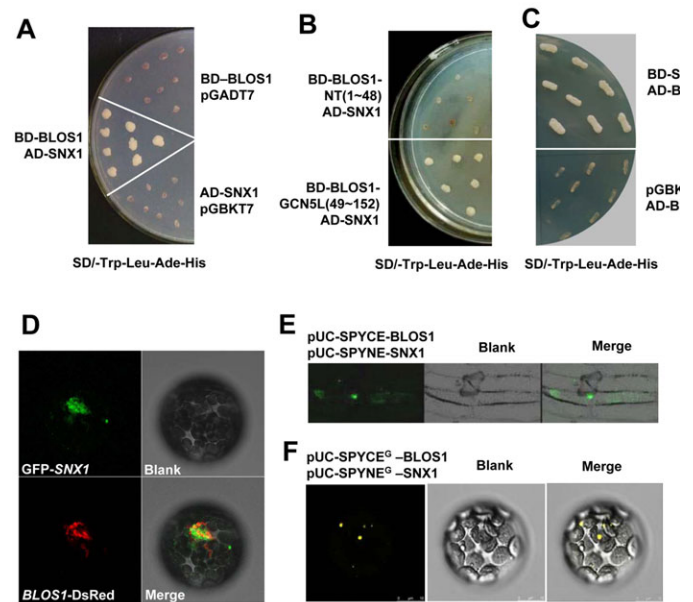
proteosomal or lysosomal protein degradation to facilitate membrane reinsertion of PIN1 and PIN2. As we showed in this study, *BLOS1* is mostly expressed in the cytosol and the transcripts of *PIN1* and *PIN2* are not significantly increased in the *BLOS1* RNAi lines (Fig. 6E); therefore, it is unlikely that BLOS1 acts as a transcription factor to regulate the expression of PIN1 and PIN2. In the FM4-64 traced assay, the endocytosis from the PM to the endosomes appears to be unaffected (Fig. 7). We have not ruled out the possibility that BLOS1 might affect the proteosomal degradation of ubiquinated PIN1 and PIN2. Based on the function of its mammalian counterpart, it is more likely that the impaired lysosomal targeting of PIN1 and PIN2 caused by the deficiency of BLOS1 might facilitate these PIN proteins to take an alternative route to the PM through membrane reinsertion. In agreement with this phenomenon, it has been reported that the melanosomal protein TYRP1 (Setty et al., 2007), the dopamine receptor D2 (Ji et al., 2009) or the NMDA receptor NR2A (Tang et al., 2009) are increased in the PM through a similar mechanism when BLOC-1 is deficient.
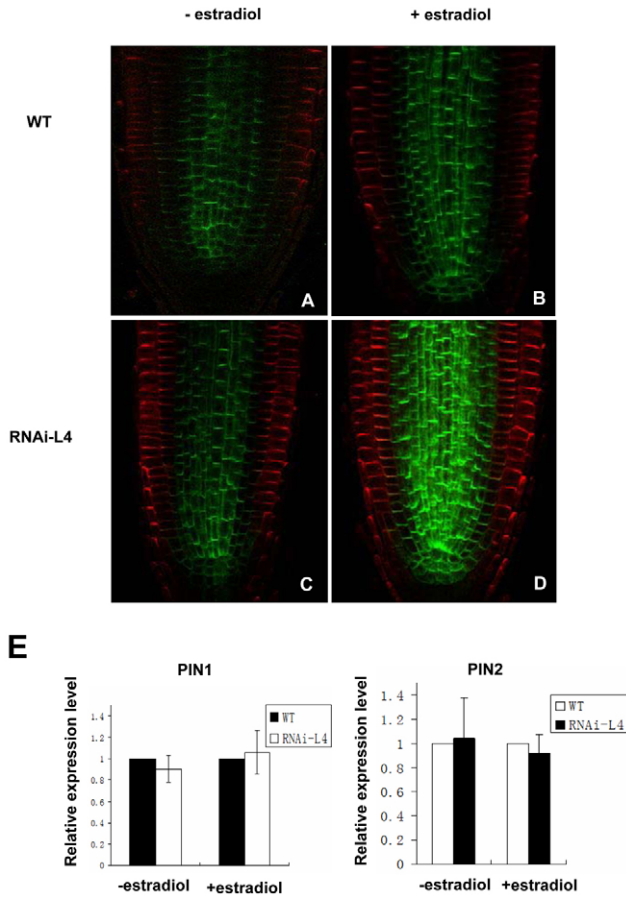
Fig. 7. Intracellular trafficking from the plasma membrane to the endosomes in *BLOS1* RNAi knockdown lines. Endocytic tracer FM4-64 binds to the membranes of endocytic compartments. FM4-64 is employed to trace intracellular trafficking from the plasma membrane to the endosomes within 15 minutes after FM4-64 uptake. No marked differences are observed in estradiol-treated *BLOS1* RNAi line (L4) compared with wild-type (WT, Col-0) and untreated lines. As a positive control, both WT and RNAi-L4 show enlarged endosomes after BFA treatment.

Fig. 6. Immunocytochemical analyses of PIN1 (green) and PIN2 (red) in *BLOS1* RNAi knockdown lines. Immunocytochemical analysis of PIN1 and PIN2 in induced and uninduced wild-type (WT, Col-0; **A**,**B**) and *BLOS1* RNAi L4 (**C**,**D**). Compared with WT and untreated lines, *BLOS1* RNAi knockdown lines (RNAi-L4) treated with 10 μM beta-estradiol have a marked increase in cells without apparent changes in polar distribution. All seedlings are 5 days old and grow vertically in the indicated medium. Seedlings are representative of at least three independent experiments and each time more than 5 seedlings are calculated. Note that all the pictures are taken with the same settings and there is no brightness difference. (**E**) Real-time PCR shows no significant increase ($P>0.05$) in the transcripts of *PIN1* and *PIN2* with 10 μM beta-estradiol inducement after normalized by the untreated lines.

BLOS1/2 with SNX1. One possible explanation is that SNX1 is responsible for the sorting of endocytosed PIN1 and PIN2 where they might be recycled to the PM via VPS29 or retromer (Jaillais et al., 2007). The recycled PIN1 and PIN2 are reduced in the *snx1* lines (Kleine-Vehn et al., 2008) and thus show the delayed root development. The opposite root phenotypes in *snx1* and in *BLOS1* RNAi lines agree with the opposite changes in PIN1 and PIN2 stability. BLOS1/2 or BLOC-1 might act in a different pathway through the interaction with SNX1 for vacuolar degradation of PIN1 and PIN2. It is possible that this proportion of PIN1 and

The timing and location of auxin accumulation determines spatiotemporal facets of developmental reprogramming. Localized increase of auxin in a single pericycle cell causes the initiation and formation of lateral roots (Dubrovsky et al., 2008). Moreover, the stabilization of PIN2 affects its abundance and distribution and leads to defects in auxin distribution and root development (Abas et al., 2006). Thus, the regulation of the homeostasis of PIN1 and PIN2 by vesicle trafficking is important to plant growth. The accumulation of PIN1 and PIN2 in the *BLOS1* RNAi lines is probably caused by impaired degradation through the endosomal-vacuole pathway, which might, in turn, lead to an increase of auxin transport that initiates the development of longer primary roots and the formation of more lateral roots.

It must be re-emphasized that the root phenotypes of *BLOS1* knockdown lines are opposite to the *snx1* lines (Jaillais et al., 2006), although we have shown the physical interaction of
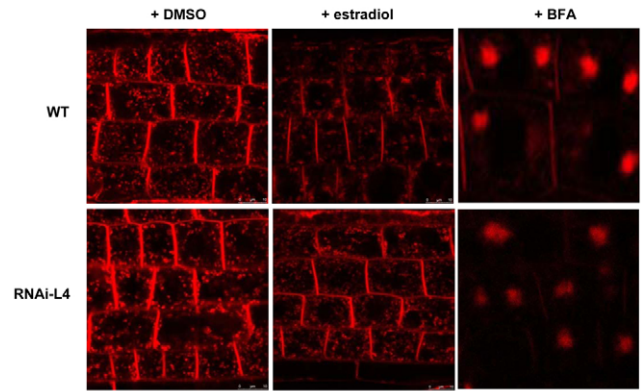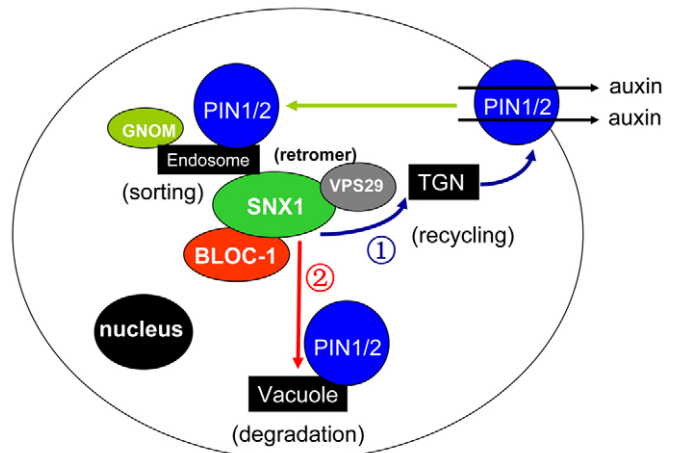

Fig. 8. A proposed model of SNX1-mediated transport of PIN proteins. In response to polar auxin transport, PIN1 and PIN2 are internalized first through the GNOM endosomes and then routed to the SNX1 endosomes for recycling. With the action of retromer, PIN1 and PIN2 are transported to the trans-Golgi network (TGN) then are reinserted into the plasma membrane (route 1). After being sorted by SNX1, PIN1 and PIN2 might be alternatively directed by BLOS1 and BLOS2 (or BLOC-1) for vacuolar degradation (route 2). SNX1 is sitting at the switch point of these two routes. When BLOC-1 is deficient or route 2 is blocked, PIN1 and PIN2 may take route 1 to be added to membrane PIN1 and PIN2.

PIN2 could be marked with mono-ubiquitin and recognized by ESCRT (Spitzer et al., 2009). To support this, our preliminary data shows that BLOC-1 interacted with ESCRT-1 in a yeast two-hybrid assay (data not shown). In the mammalian cell, it is suggested that BLOC-1 acts downstream of ESCRT (Truschel et al., 2009). Thus, we proposed a model for a dual role of SNX1, one for fast recycling of PIN1 and PIN2 via retromer (Jaillais et al., 2007) and another for vacuolar targeting of PIN1 and PIN2 via BLOC-1 (Fig. 8). Similarly, in mammalian cells, the role of SNX1 has been reported to be involved in both the retrograde endosomal transport via retromer (Gullapalli et al., 2004) and the lysosomal degradative pathway of cell surface receptors such as EGFR (Zhong et al., 2002) and PAR1 (Gullapalli et al., 2006). Our findings suggest that the vacuolar degradative pathway is important in the homeostasis of PIN1 and PIN2 to regulate the plant growth and development.

Materials and Methods
Plant growth conditions
Plants were grown under a 16:8-hour light:dark cycle at 22°C on solid Murashige and Skoog (MS) agar [half-strength MS salts, 3% (w/v) sucrose and 1% (w/v) agar]. For root analysis, seedlings were grown vertically on half MS medium in Petri dishes for the indicated period of time. For growing the inducible RNAi lines, experiments were carried out by using both wild-type (WT, Col-0) and transgenic plants treated with 10 µM beta-estradiol, whereas dimethyl sulfoxide (DMSO, a solvent for estradiol) was used as treatment for the control lines.

Yeast two-hybrid screen
The yeast two-hybrid screen was performed by following the user manual of the MATCHMAKER 3 Yeast Two-Hybrid System (Clontech, Mountain View, CA) with minor modifications. Full-length *BLOS1* cDNA (At2g30330) was amplified by PCR using the primers 5′-C<u>CATATG</u>ATGAATACGCCGATGTCACTCTC-3′ and 5′-C<u>CTGCAG</u>ACATGATGGAATCCTACTCAGGC-3′. The PCR product was cloned into the *Nde*I and *Pst*I sites of pGBKT7 (binding domain, BD) and pGADT7 (activation domain, AD) in-frame. Yeast cells were first transformed with pGBKT7-*BLOS1* and sequentially transformed with the *Arabidopsis* cDNA library constructed in the GAL4 AD vector pGAD-GH (Xie et al., 1999). The transformed cells were plated on dropout selection medium lacking Trp, Leu, His and adenine (Ade) and incubated at 30°C for 3–8 days.

To further confirm the screening results by paired yeast two-hybrid assays, full-length *BLOS2* (At5g49550) and *SNX1* (At5g06140) cDNAs were amplified with primer pairs P$_{BLOS2}$ 5′-AA<u>CATATG</u>ATGGCGGATTCACGAGATGATCTA-3′, 5′-GG<u>GAATTC</u>TCAGTCTGTAACAACAGAATCATTAG-3′ and P$_{SNX1}$ 5′-AA<u>CATATG</u>ATGGAGAGCACGGAGCAGCGAGGAA-3′, 5′-CC<u>GAATTC</u>TTAGACAGAATAAGAAGCTTCAAGTTTTGG-3′. The PCR products were respectively cloned into pGBKT7 and pGADT7 vectors in frame.

RNA interference transgenic lines
To create inducible dsRNAi transgenic lines, primers 5′-GG<u>CTCGAG</u>ACTAGT</u>ATGAATACGCCGATG-3′ and 5′-CC<u>GAATTC</u>AAG<u>CTT</u>CCATCGTCTTCATCC-3′ were used to amplify a 400 bp *BLOS1* cDNA PCR product. The remaining procedures were as described previously (Guo et al., 2003).

Western blot analysis
Two peptides LEKEKSEEESETLE and DDNRRSSLQLREKTERSRKEAI selected from BLOS1 were synthesized to generate rabbit polyclonal antibodies. The specificity of purified BLOS1 antibody from peptide DDNRRSSLQL-REKTERSRKEAI was examined in protoplast protein extracts. Expression levels of BLOS1 in different tissues were analyzed by purified BLOS1 antibody (1:4000) and protein loadings were revealed by Ponceau S staining or by tubulin. The procedures of western blotting were followed as previously described (Müller et al., 1998).

Real-time RT-PCR analysis
Real-time RT-PCR analysis (performed in MJ Bio-Rad PTC-200) was conducted by following the 'Guide to Performing Relative Quantitation of Gene Expression Using Real-Time Quantitative PCR Protocol' (Applied Biosystems, Foster City, CA). Primer pairs 5′-ACCGAGAGATCGAGAAAGGAAGCA-3′ and 5′-CGAATT-TCGCCACCGTAATGGCAA-3′ were used to detect *BLOS1* mRNA. Primer pairs for detecting *PIN1* and *PIN2* mRNA were as follows: PIN1-F: 5′-ACTC-TCAGATGCAGGTCTAGGCAT-3′; PIN1-R: 5′-ACAGTGCTAAGAATGTCAG-GATGCAC-3′; PIN2-F: 5′-CGTCCATCCTGATATTCTCAGCAC-3′; PIN2-R: 5′-CATACACCTAAGCCTGACCTGGAA-3′. Control primers for actin were 5′-GGAACTGGAATGGTGAAGGCTG-3′ and 5′-CGATTGGATACTTCAGA-GTGAGGA-3′.

Northern blotting
Total RNA from 2-week-old seedlings were isolated by the Plant RNeasy Prep Kit (Qiagen, Valencia, CA) according to the manufacturer's instructions. RNA northern blot analysis was performed (20 µg of total RNA per lane) with a ^{32}P-radiolabeled full-length BLOS1 probe. The procedure was carried out as described (Sun et al., 2003).

Bimolecular fluorescence complementation (BiFC)
The open reading frame sequences of *BLOS1*, *BLOS2* and *SNX1* were amplified by PCR with gateway-specific primer pairs Pgw$_{BLOS1}$ 5′-AAAAAGCAGGCTGGATGAATACGCCGATGTCACTC-3′, 5′-AGAAAGC-TGGGTATTGTTGATCTTCATGAATGTTTCG-3′, Pgw$_{BLOS2}$ 5′-AAAAAGCAG-GCTGGATGGCGGATTCACGAGATGA-3′, 5′-AGAAAGCTGGGTATCAGTC-TGTAACAACAGAATCATT-3′, Pgw$_{SNX1}$ 5′-AAAAAGCAGGCTGGATGGAGAG-CACGGAGCAGCCGA-3′, 5′-AGAAAGCTGGGTATTAGACAGAATAAGAA-GCTTCAAG-3′ and gateway-control primer pairs tB1 5′-GGGGACAAGT-TTGTACAAAAAAGCAGGCT3′ and tB2 5′-GGGGACCACTTTGTACAA-GAAAGCTGGGT-3′. The resulting PCR products were cloned into plasmids pUC-SPYCE-gw and pUC-DYNn-gw to give rise to pUC-SPYCE-gw-BLOS1, pUC-DYNn-gw-BLOS2 and pUC-DYNn-gw-SNX1. pUC-DYNn-gw contains N-terminal YFP modified from pUC-SPYNE-gw. To generate the gateway constructs, we followed the gateway cloning protocol (Invitrogen, Carlsbad, CA).

Histochemical localization of GUS activity
For the promoter-GUS assay, a 2187 bp genomic fragment upstream of the *BLOS1* TAA stop codon, together with a 1148 bp genomic fragment downstream of the *BLOS1* TAA stop codon, were PCR-amplified with the primer pairs P$_{2187}$ 5′-GG<u>CTGCAG</u>GGTGATCCATGTTAAAGA-3′, 5′-CC<u>GGATCC</u>TTGTTGATC-TTCATGAATG-3′ and P$_{1148}$ 5′-CC<u>GAGCTC</u>GAGCAAGTTATTGTGATTC-3′, 5′-GCC<u>GGAATTC</u>GAGAAATAAAACTTGGC-3′, respectively. The 2187 bp (*Pst*I/*Bam*HI) and 1148 bp (*Sac*I/*Eco*RI) fragments were cloned into the pBI101 vector in frame to produce the P$_{BLOS1}$-GUS fusion construct. The construct was introduced into *Arabidopsis* wild-type plants by *Agrobacterium*-mediated vacuum infiltration (Bechtold and Pelletier, 1998). After selection on MS agar plates containing 50 mg/ml kanamycin, the resulting transgenic plants were stained in GUS staining buffer (0.1% Triton X-100, 5 mM Fe^{2+}CN, 5 mM Fe^{3+}CN and 1 mg/ml X-Gluc; Sigma-Aldrich, St Louis, MO) in 50 mM sodium phosphate buffer, pH 7.0) and mounted in 50% glycerol.

Subcellular localization
A 783 bp DsRed fragment was amplified from pDsRed2N1 (Clontech) by primer pairs 5′-AGTGAACCGTCAGATCCGCTA-3′ and 5′-CCTCTAGAGTGGTATGGC-TGAT-3′. After digestion with *Kpn*I and *Xba*I, the resulting PCR product was cloned into pWM101. The *BLOS1* and *BLOS2* cDNAs were amplified from wild-type Columbia (Col-0) with the primers 5′-CGAGAGCTCATGAATACGCCGATGT-CAC-3′, 5′-TGCGGTACCTGTTGATCTTCATGAATGTT-3′ and 5′-GAGAGCT-CATGGCGGATTCACGAGATGATCTAGCTG-3′, 5′-GAGGTACCCTGTAACA-ACAGAATCATTAGAGCGACGC-3′, respectively. The PCR products were cloned into the *Sac*I/*Kpn*I sites of the CaMV35S:DsRed2N1:pWM101vector. *SNX1* was amplified by the primers 5′-TGTGAGCTCATGGAGAGCACGGAGCAGCC-3′ and 5′-ACCGGTACCACAGAATAAGAAGCTTCAAGT-3′. The PCR products were cloned into the *Sac*I/*Kpn*I sites of the CaMV35S:GFP:pWM101 vector. The resulting constructs were introduced into *Arabidopsis* protoplast as described (Hwang and Sheen, 2001).

Immunocytochemical analysis
Immunocytochemical analysis of PIN1 and PIN2 was performed on whole-mount roots of 5-day-old seedlings. Mouse anti-PIN1 (Gälweiler et al., 1998) and guinea pig anti-PIN2 (Müller et al., 1998) were diluted to 1:50 and 1:100, respectively. For the secondary antibodies, Alexa Fluor 488 goat anti-mouse IgG and Alexa Fluor 555 goat anti-guinea pig IgG (Invitrogen) were diluted to 1:500. The detailed procedures were previously described (Friml et al., 2002a; Friml et al., 2002b). Imaging was performed using a Zeiss LSM 510 Meta inverted confocal microscope and accompanying software.

For FM4-64 treatments, seedlings were incubated for 15 minutes at room temperature in half-liquid medium containing FM4-64 (5 µM) and rinsed three times in half-liquid medium. BFA (25 µM in DMSO) treatments were performed in half-liquid medium for 1 hour before observation.

Statistics
Quantitative data in paired groups was analyzed using the Student's *t*-test. Qualitative data was compared using the χ^2 test.

Accession numbers
Sequence data from this article can be found in the EMBL and GenBank data libraries under the following accession numbers: *BLOS1* (At2g30330, NM_128586), *BLOS2* (At5g49550, NM_124332) and *SNX1* (At5g06140, NM_120696). The accession numbers of the homologs of BLOS1 and BLOS2 are listed in Fig. S1 in the supplementary material.

Supplementary material available online at
http://jcs.biologists.org/cgi/content/full/123/21/3727/DC1

References

Abas, L., Benjamins, R., Malenica, N., Paciorek, T., Wisniewska, J., Moulinier-Anzola, J. C., Sieberer, T., Friml, J. and Luschnig, C. (2006). Intracellular trafficking and proteolysis of the Arabidopsis auxin-efflux facilitator PIN2 is involved in root gravitropism. *Nat. Cell Biol.* **8**, 249-256.

Baluska, F., Hlavacka, A., Samaj, J., Palme, K., Robinson, D. G., Matoh, T., McCurdy, D. W., Menzel, D. and Volkmann, D. (2002). F-actin-dependent endocytosis of cell wall pectins in meristematic root cells. Insights from brefeldin A-induced compartments. *Plant Physiol.* **130**, 422-431.

Bechtold, N. and Pelletier, G. (1998). In *planta* Agrobacterium mediated transformation of adult *Arabidopsis thaliana* plants by vacuum infiltration. *Methods Mol. Biol.* **82**, 259-266.

Bonifacino, J. S. and Glick, B. S. (2004). The mechanisms of vesicle budding and fusion. *Cell* **116**, 153-166.

Bonifacino, J. S. and Rojas, R. (2006). Retrograde transport from endosomes to the trans-Golgi network. *Nat. Rev. Mol. Cell Biol.* **7**, 568-579.

Dhonukshe, P., Aniento, F., Hwang, I., Robinson, D. G., Mravec, J., Stierhof, Y.-D. and Friml, J. (2007). Clathrin-mediated constitutive endocytosis of PIN auxin efflux carriers in *Arabidopsis*. *Curr. Biol.* **17**, 520-527.

Dhonukshe, P., Tanaka, H., Goh, T., Ebine, K., Mähönen, A. P., Prasad, K., Blilou, I., Geldner, N., Xu, J., Uemura, T. et al. (2008). Generation of cell polarity in plants links endocytosis, auxin distribution and cell fate decisions. *Nature* **456**, 962-966.

Dubrovsky, J. G., Sauer, M., Napsucialy-Mendivil, S., Ivanchenko, M., Friml, J., Shishkova, S., Celenza, J. and Benková, E. (2008). Auxin acts as a local morphogenetic trigger to specify lateral root founder cells. *Proc. Natl. Acad. Sci. USA* **105**, 8790-8794.

Frigerio, L., Hinz, G. and Robinson, D. G. (2008). Multiple vacuoles in plant cells: rule or exception? *Traffic* **9**, 1564-1570.

Friml, J., Benková, E., Blilou, I., Wisniewska, J., Hamann, T., Ljung, K., Woody, S., Sandberg, G., Scheres, B., Jürgens, G. et al. (2002a). AtPIN4 mediates sink driven auxin gradients and root patterning in Arabidopsis. *Cell* **108**, 661-673.

Friml, J., Wisniewska, J., Benková, E., Mendgen, K. and Palme, K. (2002b). Lateral relocation of auxin efflux regulator PIN3 mediates tropism in Arabidopsis. *Nature* **415**, 806-809.

Gälweiler, L., Guan, C., Müller, A., Wisman, E., Mendgen, K., Yephremov, A. and Palme, K. (1998). Regulation of polar auxin transport by AtPIN1 in Arabidopsis vascular tissue. *Science* **282**, 2226-2230.

Geldner, N., Friml, J., Stierhof, Y., Jurgens, G. and Palme, K. (2001). Auxin transport inhibitors block PIN1 cycling and vesicle trafficking. *Nature* **413**, 425-428.

Geldner, N., Anders, N., Wolters, H., Keicher, J., Kornberger, W., Muller, P., Delbarre, A., Ueda, T., Nakano, A. and Jurgens, G. (2003). The Arabidopsis GNOM ARF-GEF mediates endosomal recycling, auxin transport, and auxin dependent plant growth. *Cell* **112**, 219-230.

Goh, T., Uchida, W., Arakawa, S., Ito, E., Dainobu, T., Ebine, K., Takeuchi, M., Sato, K., Ueda, T. and Nakano, A. (2007). VPS9a, the common activator for two distinct types of Rab5 GTPases, is essential for the development of Arabidopsis thaliana. *Plant Cell* **19**, 3504-3515.

Gruenberg, J. (2001). The endocytic pathway: a mosaic of domains. *Nat. Rev. Mol. Cell Biol.* **2**, 721-730.

Gullapalli, A., Garrett, T. A., Paing, M. M., Griffin, C. T., Yang, Y. and Trejo, J. (2004). A role for sorting nexin 2 in epidermal growth factor receptor down-regulation: evidence for distinct functions of sorting nexin 1 and 2 in protein trafficking. *Mol. Biol. Cell* **15**, 2143-2155.

Gullapalli, A., Wolfe, B. L., Griffin, C. T., Magnuson, T. and Trejo, J. (2006). An essential role for SNX1 in lysosomal sorting of protease-activated receptor-1: evidence for retromer-, Hrs-, and Tsg101-independent functions of sorting nexins. *Mol. Biol. Cell* **17**, 1228-1238.

Guo, H. S., Fei, J. F., Xie, Q. and Chua, N. H. (2003). A chemical-regulated inducible RNAi system in plants. *Plant J.* **34**, 383-392.

Hwang, I. and Sheen, J. (2001). Two-component circuitry in Arabidopsis cytokinin signal transduction. *Nature* **41**, 3383-3389.

Iizuka, Y., Sei, Y., Weinberger, D. R. and Straub, R. E. (2007). Evidence that the BLOC-1 protein dysbindin modulates dopamine D2 receptor internalization and signaling but not D1 internalization. *J. Neurosci.* **27**, 12390-12395.

Jaillais, Y., Fobis-Loisy, I., Miège, C., Rollin, C. and Gaude, T. (2006). AtSNX1 defines an endosome for auxin-carrier trafficking in Arabidopsis. *Nature* **443**, 106-109.

Jaillais, Y., Santambrogio, M., Rozier, F., Fobis-Loisy, I., Miege, C. and Gaude, T. (2007). The retromer protein VPS29 links cell polarity and organ initiation in plants. *Cell* **130**, 1057-1070.

Jaillais, Y., Fobis-Loisy, I., Miège, C. and Gaude, T. (2008). Evidence for a sorting endosome in Arabidopsis root cells. *Plant J.* **53**, 237-247.

Jauh, G. Y., Fischer, A. M., Grimes, H. D., Ryan, C. A., Jr and Rogers, J. C. (1998). delta-Tonoplast intrinsic protein defines unique plant vacuole functions. *Proc. Natl. Acad. Sci. USA* **95**, 12995-12999.

Jauh, G. Y., Phillips, T. E. and Rogers, J. C. (1999). Tonoplast intrinsic protein isoforms as markers for vacuolar functions. *Plant Cell* **11**, 1867-1882.

Ji, Y., Yang, F., Papaleo, F., Wang, H. X., Gao, W. J., Weinberger, D. R. and Lu, B. (2009). Role of dysbindin in dopamine receptor trafficking and cortical GABA function. *Proc. Natl. Acad. Sci. USA* **106**, 19593-19598.

Kleine-Vehn, J., Leitner, J., Zwiewka, M., Sauer, M., Abas, L., Luschnig, C. and Friml, J. (2008). Differential degradation of PIN2 auxin efflux carrier by retromer-dependent vacuolar targeting. *Proc. Natl. Acad. Sci. USA* **105**, 17812-17817.

Kornfeld, S. and Mellman, I. (1989). The biogenesis of lysosomes. *Annu. Rev. Cell Biol.* **5**, 483-525.

Laxmi, A., Pan, J., Morsy, M. and Chen, R. (2008). Light plays an essential role in intracellular distribution of auxin efflux carrier PIN2 in Arabidopsis thaliana. *PLoS ONE* **3**, e1510.

Li, W., Zhang, Q., Oiso, N., Novak, E. K., Gautam, R., O'Brien, E. P., Tinsley, C. L., Blake, D. J., Spritz, R. A., Copeland, N. G. et al. (2003). Hermansky-Pudlak syndrome type 7 (HPS-7) results from mutant dysbindin, a member of the biogenesis of lysosome-related organelles complex 1 (BLOC-1). *Nat. Genet.* **35**, 84-89.

Li, W., Feng, Y. Q., Hao, C. J., Guo, X. L., Cui, Y. Y., He, M. and He, X. (2007). The BLOC interactomes form a network in endosomal transport. *J. Genet. Genomics* **34**, 669-682.

Morgan, N. V., Pasha, S., Johnson, C. A., Ainsworth, J. R., Eady, R. A., Dawood, B., McKeown, C., Trembath, R. C., Wilde, J., Watson, S. P. et al. (2006). A germline mutation in BLOC1S3/ reduced pigmentation causes a novel variant of Hermansky-Pudlak syndrome (HPS8). *Am. J. Hum. Genet.* **78**, 160-166.

Müller, A., Guan, C., Gälweiler, L., Tänzler, P., Huijser, P., Marchant, A., Parry, G., Bennett, M., Wisman, E. and Palme, K. (1998). AtPIN2 defines a locus of *Arabidopsis* for root gravitropism control. *EMBO J.* **17**, 6903-6911.

Müller, J., Mettbach, U., Menzel, D. and Samaj, J. (2007). Molecular dissection of endosomal compartments in plants. *Plant Physiol.* **145**, 293-304.

Paciorek, T., Zazimalova, E., Ruthardt, N., Petrasek, J., Stierhof, Y.-D., Kleine-Vehn, J., Morris, D. A., Emans, N., Jurgens, G., Geldner, N. et al. (2005). Auxin inhibits endocytosis and promotes its own efflux from cells. *Nature* **435**, 1251-1256.

Raposo, G., Marks, M. S. and Cutler, D. F. (2007). Lysosome-related organelles: driving post-Golgi compartments into specialisation. *Curr. Opin. Cell Biol.* **19**, 394-401.

Setty, S. R., Tenza, D., Truschel, S. T., Chou, E., Sviderskaya, E. V., Theos, A. C., Lamoreux, M. L., Di Pietro, S. M., Starcevic, M., Bennett, D. C. et al. (2007). BLOC-1 is required for cargo-specific sorting from vacuolar early endosomes toward lysosome-related organelles. *Mol. Biol. Cell* **18**, 768-780.

Shen, B., Li, C., Min, Z., Meeley, R. B., Tarczynski, M. C. and Olsen, O.-A. (2003). Sal1 determines the number of aleurone cell layers in maize endosperm and encodes a class E vacuolar sorting protein. *Proc. Natl. Acad. Sci. USA* **100**, 6552-6557.

Silady, R. A., Kato, T., Lukowitz, W., Sieber, P., Tasaka, M. and Somerville, C. R. (2004). The gravitropism defective 2 mutants of Arabidopsis are deficient in a protein implicated in endocytosis in Caenorhabditis elegans. *Plant Physiol.* **136**, 3095-3103.

Silady, R. A., Ehrhardt, D. W., Jackson, K., Faulkner, C., Oparka, K. and Somerville, C. R. (2008). The GRV2/RME-8 protein of Arabidopsis functions in the late endocytic pathway and is required for vacuolar membrane flow. *Plant J.* **53**, 29-41.

Spitzer, C., Reyes, F. C., Buono, R., Sliwinski, M. K., Haas, T. J. and Otegui, M. S. (2009). The ESCRT-related CHMP1A and B proteins mediate multivesicular body sorting of auxin carriers in Arabidopsis and are required for plant development. *Plant Cell* **21**, 749-766.

Steinmann, T., Geldner, N., Grebe, M., Mangold, S., Jackson, C. L., Paris, S., Gälweiler, L., Palme, K. and Jürgens, G. (1999). Coordinated polar localization of auxin efflux carrier PIN1 by GNOM ARF GEF. *Science* **286**, 316-318.

Sun, J., Niu, Q. W., Tarkowski, P., Zheng, B., Tarkowska, D., Sandberg, G., Chua, N. H. and Zuo, J. (2003). The *Arabidopsis* AtIPT8/PGA22 gene encodes an isopentenyl transferase that is involved in de novo cytokinin biosynthesis. *Plant Physiol.* **131**, 167-176.

Tang, T. T., Yang, F., Chen, B. S., Lu, Y., Ji, Y., Roche, K. W. and Lu, B. (2009). Dysbindin regulates hippocampal LTP by controlling NMDA receptor surface expression. *Proc. Natl. Acad. Sci. USA* **106**, 21395-21400.

Tian, Q., Olsen, L., Sun, B., Lid, S. E., Brown, R. C., Lemmon, B. E., Fosnes, K., Gruis, D., Opsahl-Sorteberg, H.-G., Otegui, M. S. et al. (2007). Subcellular localization and functional domain studies of DEFECTIVE KERNEL1 in maize and Arabidopsis suggest a model for aleurone cell fate specification involving CRINKLY4 and SUPERNUMERARY ALEURONE LAYER1. *Plant Cell* **19**, 3127-3145.

Truschel, S. T., Simoes, S., Setty, S. R., Harper, D. C., Tenza, D., Thomas, P. C., Herman, K. E., Sackett, S. D., Cowan, D. C., Theos, A. C. et al. (2009). ESCRT-I function is required for Tyrp1 transport from early endosomes to the melanosome limiting membrane. *Traffic* **10**, 1318-1336.

Xie, Q., Sanz-Burgos, A. P., Guo, H., Garcia, J. A. and Gutierrez, C. (1999). GRAB proteins, novel members of the NAC domain family, isolated by their interaction with a geminivirus protein. *Plant Mol. Biol.* **39**, 647-656.

Zhong, Q., Lazar, C. S., Tronchère, H., Sato, T., Meerloo, T., Yeo, M., Songyang, Z., Emr, S. D. and Gill, G. N. (2002). Endosomal localization and function of sorting nexin 1. *Proc. Natl. Acad. Sci. USA* **99**, 6767-6772.